Asociación Argentina
de Mecánica Computacional

Mecánica Computacional Vol XXXII, págs. 631-645 (artículo completo)
Carlos G. García Garino, Aníbal E. Mirasso, Mario A. Storti, Miguel E. Tornello (Eds.)
Mendoza, Argentina, 19-22 Noviembre 2013

STRUCTURAL BEHAVIOR OF TIMBER BEAMS WITH A MODULUS OF ELASTICITY REPRESENTED BY A RANDOM FIELD

Diego A. García[a,b,c], Juan Carlos J. Piter[d], Mario R. Escalante[e] and Marta B. Rosales[a,c]

[a]*Departamento de Ingeniería, Universidad Nacional del Sur, Av. Alem 1253, 8000 Bahía Blanca, Argentina, garciadiego@fio.unam.edu.ar, mrosales@criba.edu.ar.*

[b]*Departamento de Ingeniería Civil, Universidad Nacional de Misiones, Juan Manuel de Rosas 325, 3360 Oberá, Argentina.*

[c]*CONICET, Argentina.*

[d]*Grupo de Estudio de Maderas (GEMA), Departamento de Ingeniería Civil, FRCU-UTN, Ing. Pereyra 676, 3260 Concepción del Uruguay, Argentina, piterj@frcu.utn.edu.ar.*

[e]*Grupo de Métodos Numéricos, FRCU-UTN, Ing. Pereyra 676, 3260 Concepción del Uruguay, Argentina, mrescalante@frcu.utn.edu.ar.*

Keywords: Random field, modulus of elasticity, timber beams, midspan deflection.

Abstract. A stochastic model of the structural behavior of a $Eucalyptus\ grandis$ timber beam is herein presented. Three strength classes obtained according to the the criterion of the Argentinean standard IRAM 9662-2:2006 are studied. The Modulus of Elasticity (MOE) is considered as a random field. The MOE uncertainties are quantified in the beam deflection and the random field is given by a gamma probability density function (PDF) and an exponential correlation function. Experimental data obtained from bending tests performed with 349 sawn beams of Argentinean $Eucalyptus\ grandis$ are employed to find the PDF parameters. Statistical results of the deflection are reported for the case of pure bending of a simply supported beam. Focus is made on the central deflection. The methodology was previously verified comparing with some results published by other authors. The influence of the correlation length is assessed for limiting and intermediate cases. The problem is solved by a discretization with a finite element model and the Nataf transform is employed in order to generate and simulate the random field. Additionally, the random field is discretized by means of the Midpoint Method. Numerical results are obtained by means of Monte Carlo simulations and previously a convergence study was carried out to determine the number of realizations that gives a reasonable accuracy. The PDF and cumulative distribution function (CDF) of the central deflection allows obtaining statistical estimates. As a particular case, the homogeneous model with the MOE assumed as a random variable is studied with some detail. The propagation is made analytically and the explicit PDF of the central deflection is obtained. Since wood is a material with very variable mechanical properties, assuming the MOE as a random field contributes to attain a more realistic structural model. In particular, the study of the correlation length variability also provides a larger amount of information about the range of the response. It should be noted that within the standard code in use, the MOE is eventually modeled as a random variable and not as a random field. It is shown that the MOE modeled as a random variable constitutes a more conservative approach.

1 INTRODUCTION

Due to its natural origin, structural timber is characterized by considerable lengthwise variability in its mechanics properties. However these properties are treated as random variables and their spatial variability is not taken into account in design practice. Owing to the specific structure of trunk and branches, the structural timber can be characterized as a composition of clear wood and growth defects. Clear wood is an anisotropic material, but its properties do not change considerably along grains. On the other hand, growth defects such as knots, often related to localized grain deviations, are the main source of the lengthwise variability of bending strength and stiffness in timber beams. The presence of grain deviations can decrease the MOE in the longitudinal direction. Since knots are unavoidable in structural timber, the effective MOE in the longitudinal direction varies along the main axis of a beam.

Eucalyptus grandis, which is mainly cultivated in the Mesopotamian provinces of Entre Rios and Corrientes, is one of the most important renewable species cultivated in Argentina (INTA, 1995). A simple method for visually strength grading sawn timber of these species has been developed by Piter (2003). According to Piter, the presence of pith, or medulla, often associated with other defects as fissures, significantly reduces the strength and the stiffness of this sawn timber. This feature is also considered the most important visual characteristic for strength grading this material by the Argentinean standard IRAM:9662-2 (2006). Other important features taken into account as grading are the knot ratio and grain deviation (Piter (2003) and IRAM:9662-2 (2006)).

Due to the variability in their mechanical properties, in particular the lengthwise variability of MOE, a stochastic approach is necessary in order to attain a more realistic structural model. Therefore, a realistic response of structural components subjected to external demands is desirable.

The lengthwise variation of MOE, was modeled by Czmoch (1998) as a stationary random process. He studied the midspan deflection in *Pine spruce* beams and applied several PDF of MOE. Point discretization methods and Nataf transform were applied, in order to carried out a reliability analysis of the serviceability limit state. Furthermore, both an experimental and numerical study of the scale of fluctuation and its incidence in the structural element response are presented. Escalante et al. (2012), study the buckling of Eucalyptus grandis wood columns and model the lengthwise variation of MOE as a Normal random process. They also applied Karhunen-Loeve (KL) expansion in order to discretize the random field. Köhler et al. (2007) present a probabilistic model of timber structures where the MOE is modeled as a random variable with Lognormal PDF, assuming a homogeneous value within a structural element. Then, Köhler (2007), presents a discrete model of the lengthwise variability of MOE, following the model proposed for bending moment capacity reported by Isaksson (1999). In this model, the discrete section transition is assumed to be Poisson distributed, thus the section length follows an exponential distribution.

Der Kiureghian and Liu (1986), introduce the Nataf transform, applied to the structural reliability under incomplete probability information on random variables. Ditlevsen and Madsen (1996), present this transformation in their book of reliability methods.

The aim of this work is to quantify the influence of the lengthwise variability of MOE, in the midspan deflection (V(L/2)) of simply supported *Eucalyptus grandis* beams. To accomplish this, the PDF and CDF of the midspan deflection was found via Monte Carlo simulations, Rubinstein (1981). The influence of the lengthwise variability of MOE in the structural component response, is determined for the values of the scale of fluctuation of the random field. The study

of the correlation length variability, also provides a large amount of information about the range of the response. In order to quantify this influence, we applied to $Eucalyptus\ grandis$ beams the methodology presented by Czmoch (1998). The problem is analyzed by means a discretization with a finite element model. The random field is generated, from the correlation function and the PDF of MOE through the Nataf transform. The random field is discretized in order to apply the material properties to the finite element model and to find the probability density function of V(L/2) (f[V(L/2]) and its cumulative density function (F[V(L/2)]) by means of independent Monte Carlo simulations. The PDF of MOE is obtained by means of the Principle of Maximum Entropy (Shannon, 1948), and its parameters by means of the maximum likelihood method (MLM) applied to MOE values that were obtained experimentally. In order to measure the fit between experimental and theoretical PDF of MOE the Kolmogorov-Smirnov (K-S) test of fit is used.

Next, MOE modeled as a random variable is studied numerically and analytically. Differences between MOE assumed as a random variable and as a random field are presented and discussed. Finally, a comparison between results of numerical simulations of a bending test and results of a bending test obtained experimentally is also presented.

2 STATEMENT OF PROBLEM

In this work, we present the study of the midspan deflection of a simply supported Eucalyptus grandis timber beam, with stochastic bending stiffness subjected to pure bending, as shown in Figure 1.

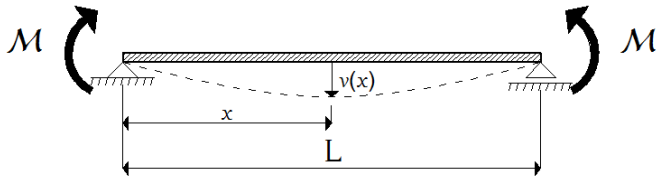

Figure 1: Deflection of simply supported beam subjected to pure bending.

The following differential equation, describes the relationship between the beam's deflections $v(x)$ at some position x and the bending moment for a Euler-Bernoulli beam:

$$ei(x)\frac{d^2v(x)}{dx^2} = -\mathcal{M} \tag{1}$$

where $\mathcal{M}$ is the bending moment constant along the beam; i is the second moment of area of the beam's cross section; e is the Modulus of Elasticity (MOE) and $ei(x)$ is the deterministic bending stiffness at some position x.

In the present work, the lengthwise variability of the MOE is represented by means of the random field $E(x)$; assuming deterministic values for the cross section and the applied bending moment. In what follows, the random quantities are denoted by capital letters. The random deflection field $V(x)$ and the deterministic bending moment are related as follows:

$$E(x)i\frac{d^2V(x)}{dx^2} = -\mathcal{M} \tag{2}$$

We define the homogeneous random field $\{E(x) : x \in [0; L]\}$ as a collection of real-valued random variables from a probability space $(\Omega, \mathcal{F}, P)$, where Ω is the sample space, $\mathcal{F}$ is the σ-algebra and P is the probability measure.

3 STOCHASTIC FINITE ELEMENT PROCEDURE

In order to find the PDF of the midspan deflection f[V(L/2)], Eq. (2) is discretized by means of the finite element method, ($e.g.$ Bathe (1996)). Bernoulli beam elements with two nodes and two degrees of freedom per node are employed. These elements are based in the following shape functions:

$$v(x) = \mathbf{n}^T(x)\mathbf{v}. \tag{3}$$

where

$$\mathbf{v}^T = \begin{bmatrix} v_1 & \theta_1 & v_2 & \theta_2 \end{bmatrix} \tag{4}$$

is a vector of beam element nodal displacement, as shown in Figure 2, and,

$$\mathbf{n}(x) = \begin{bmatrix} 1 & 0 & \dfrac{3}{L_e^2} & \dfrac{2}{L_e^3} \\ 0 & 1 & \dfrac{2}{L_e} & \dfrac{1}{L_e} \\ 0 & 0 & \dfrac{3}{L_e^2} & -\dfrac{2}{L_e^3} \\ 0 & 0 & \dfrac{1}{L_e} & \dfrac{1}{L_e^2} \end{bmatrix} \begin{bmatrix} 1 \\ x \\ x^2 \\ x^3 \end{bmatrix} \tag{5}$$

where L_e is the element length. Then, in order to apply the material properties in the beam

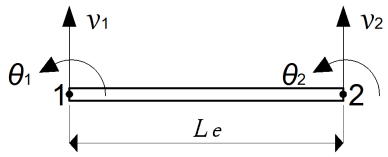

Figure 2: Bernoulli beam finite element with 4 degree of freedom.

elements, it is necessary to mesh the random field. To do this, in this work we use a discretization method which belongs to a family of point discretization methods. In these methods, the material property is constant within a random field element and it is a single random variable. The midpoint method consists in associating a random variable, to the centroid of each element of the mesh, and representing the field in each point of the element by this random variable.

In the midpoint method, a random field $E(x)$ is represented by a set of random variables, defined for random field elements matching with the finite elements, as follows:

$$E_i = E(x_c^{(i)}) \tag{6}$$

where $x_c^{(i)}$ is the location of the centroid of the i-th element.

The mean value of random variable E_i is given as:

$$\mathbf{E}[E_i] = \mathbf{E}[E(x_c^{(i)})] \tag{7}$$

and the covariance between random variables E_i, E_j is equal to

$$\mathbf{Cov}[E_i, E_j] = \mathbf{C}_E(x_c^{(i)}, x_c^{(j)}) \tag{8}$$

where $\mathbf{C}_E(x_c^{(i)}, x_c^{(j)})$ is the covariance function of random field.

In the midpoint discretization method, the distribution of the random variable E_i remains the same as the first-order distribution of the random field $E(x)$:

$$F_{E_i}(e_i) = P[E(x_c^{(i)}) \leq e_i] = F_E(e_i(x_c^{(i)})) \tag{9}$$

which for an homogeneous and stationary random field, does not depend on the location of the centroid of the i-th element. The midpoint method is suitable for discretization of non-Gaussian random field, Czmoch (1998).

Based on the midpoint discretization method, and the beam element shape function previously presented, the following beam element stiffness matrix is obtained:

$$k_e = \frac{Ei}{L_e^3}\begin{bmatrix} 12 & 6L_e & -12 & 6L_e \\ 6L_e & 4L_e^2 & -6L_e & 2L_e^2 \\ -12 & -6L_e & 12 & -6L_e \\ 6L_e & 2L_e^2 & -6L_e & 4L_e \end{bmatrix} \tag{10}$$

Next, the global matrix can be obtained with the usual finite element assembling and the beam deformation is calculated from the equation:

$$\mathbf{KV} = \mathbf{Q} \tag{11}$$

where $\mathbf{K}$ is the n x n positive-definite global stiffness matrix, $\mathbf{V}$ is the n x 1 vector of global nodal displacement, and $\mathbf{Q}$ is the n x 1 vector of global nodal forces.

4 RANDOM FIELD OF THE MOE

The Nataf transform is employed in order to generate and simulate the random field of MOE. It has been introduced in the field of structural engineering by Der Kiureghian and Liu (1986). It allows to build a multidimensional PDF that fits some prescribed marginal distributions and some correlation matrix.

Suppose a random vector X has prescribed marginal distributions, say $F_{X_i}(x_i), i = 1, \ldots, M$ and a correlation matrix R. It is possible to transform the components of X into standard normal random variables $\xi_i, i = 1, \ldots, M$:

$$\xi_i = \Phi^{-1}(F_{X_i}(x_i)) \tag{12}$$

The Nataf transform assumes that $\Xi = \{\xi_1, \ldots, \xi_M\}^T$ is a standard normal correlated vector whose joint PDF reads:

$$f_\Xi(\xi_1, \ldots, \xi_M) = \varphi_M(\xi; R_0) \tag{13}$$

where $\varphi_M(\xi; R_0)$ is the multidimensional normal PDF:

$$\varphi_M(\xi; R_0) = \frac{1}{\sqrt{(2\pi)^M det R_0}} exp\left[-\frac{1}{2}\xi^T R_0^{-1}\xi\right] \tag{14}$$

and R_0 is a correlation matrix (corresponding to the multidimensional normal PDF) that should be compatible with the prescribed correlation matrix R (corresponding to the random field of the prescribed marginal distribution). From the above equations, one can write:

$$f_X(x_1, \ldots, x_M) = f_\Xi(\xi_1, \ldots, \xi_M)\,|det \mathcal{J}_{\Xi,X}| \tag{15}$$

where the Jacobian of the transform is a diagonal matrix:

$$\mathcal{J}_{\Xi,X} = diag\left(\frac{f_{X_1}(x_1)}{\varphi(\xi_1)}, \ldots, \frac{f_{X_M}(x_M)}{\varphi(\xi_M)}\right) \tag{16}$$

this leads to the Nataf transform

$$f_X(x_1, \ldots, x_M) = \prod_{i=1}^{M} \frac{f_{X_i}(x_i)}{\varphi(\xi_i)} \varphi_M(\xi; R_0) \tag{17}$$

The correlation matrix R_0, is computed term by term by solving the following consistency equation for ρ_{ij}:

$$\rho_{ij} = \int_{-\infty}^{\infty}\int_{-\infty}^{\infty} \left(\frac{x_i - \mu_{X_i}}{\sigma_{X_i}}\right)\left(\frac{x_j - \mu_{X_j}}{\sigma_{X_j}}\right) \varphi_2(\xi_i, \xi_j; \rho_{0ij}) d\xi_i d\xi_j \tag{18}$$

where ρ_{ij} and ρ_{0ij} are the non-dimensional correlation matrix elements. Due to the burden of such a computation in the general case, values of $\kappa = \frac{\rho_{0ij}}{\rho_{ij}}$ have been tabulated for various couples of distributions $(f_{X_i}(x_i), f_{X_j}(x_j))$ in Der Kiureghian and Liu (1986) and Ditlevsen and Madsen (1996).

4.1 Marginal PDF of the MOE

If a stochastic approach is applied to this problem, first a PDF should be chosen for the input variable. A statistical concept of entropy was introduced by Shannon (1948). He derived the Principle of Maximum Entropy which states that, subject to known constrains, the PDF which best represents the current state of knowledge is the one with largest entropy. The measure of uncertainties of a random variable X is defined by the following expression

$$S(f_X) = -\int_D f_X(X) log(f_X(X)) dX \tag{19}$$

in which f_X stands for the PDF of X and D is its domain.

It is possible to demonstrate the application of the principle under the constraints of positiveness and bounded second moment, leads to a gamma PDF. This is due to the domain of MOE is positive real, $E_i \in]0, \infty[$, and the interval is open, $i.e.$ the boundaries do not belong to the interval.

To find the parameters of the marginal PDF of MOE, experimental data presented by Piter (2003), obtained by means of two point load bending tests, performed with 349 sawn beams of Argentinean $Eucalyptus\ grandis$ with structural dimensions, are employed. Bending tests were carried out according to UNE-EN408 (1995), Figure 3, and the worst defects were placed in the constant bending zone, between two concentrated loads and in the tensile region of the cross section. This values of the MOE were calculated taking into account the shear deformation (global MOE). Therefore, values of the MOE experimentally obtained are classified according to the strength classes established for the visual grading of the $Eucalyptus\ grandis$ cultivated in the Mesopotamian provinces of Argentina by the standard IRAM:9662-2 (2006), see Table 1 and Table 2.

Values of the MOE experimentally obtained were corrected to a uniform moisture content of 12%, in order to make comparable the 349 values that have been calculated of beams with different humidity content. This humidity content is a standard reference value established in

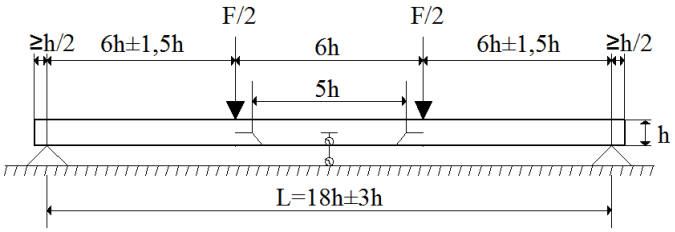

Figure 3: Two point loads bending test according to UNE-EN 408.

Strength class	Presence of pith	Knot ratio	Grain deviation
C1	No	K$\leq 1/3$	gd<$1/12$
C2	No	$1/3$<K$\leq 2/3$	gd<$1/9$
C3	Yes	$2/3$<K	$1/9$<gd

Table 1: *Eucalyptus grandis* strength classes, according to IRAM 9662-2:2006.

the normative. The humidity content previously established, corresponds to at a temperature of 20°C and a relative humidity of 65%. The values of global MOE (E_g) obtained with experimental data have been corrected, increasing in 2% for each 1% in excess to the standardized condition of 12% of humidity content, and vice verse, in each timber beam. On the other hand with the following expression, 349 values of E_g has been calculated and reported by Piter (2003)

$$E_g = \frac{L^3 \left(F_2 - F_1\right)}{4.7bh^3(w_2 - w_1)} \tag{20}$$

where $(F_2 - F_1)$ is the load increment and $(w_2 - w_1)$ is the midspan deflection increment corresponding to the load increment. This load increment is within the linear elastic range of the material.

Since structural timber beams are composed of clear wood, where the MOE can take higher values, and wood with defects, where MOE is reduced, we adopted a criteria to determine the PDF parameters, as shown in Table 3.

The parameters of the marginal PDF of the MOE are estimated with the help of the maximum likelihood method (MLM). Finally, the Kolmogorov-Smirnov (K-S) test of fit is used (*e.g.* Benjamin and Cornell (1970)). The level of significance α of the parametric hypothesis is assumed to be 0,05. For α=0,05 the critical value for the Kolmogorov-Smirnov test of fit is equal to c=1,36. Results of test of fit are presented in Table 4.

The gamma marginal PDF of the MOE is:

$$f(x \mid a, b) = \frac{1}{b^a \Gamma(a)} x^{a-1} e^{-\frac{x}{b}} \tag{21}$$

Strength class	Number of MOE measurements
C1	119
C2	62
C3	168

Table 2: Composition of MOE measurements, experimentally obtained.

Grade	Presence of pith	Knot ratio	Grain deviation	Number of MOE measurements
Grade1	No	K$\leq 1/3$	gd<$1/12$	119
Grade2	No	K$\leq 2/3$	gd<$1/9$	181
Grade3	Yes	$2/3$<K	$1/9$<gd	349

Table 3: Classification in grades of MOE values.

Grade	Kolmogorov-Smirnov $D\sqrt{n}$ Statistics	Significance test
Grade 1	0,48	0,48<1,36
Grade 2	0,41	0,41<1,36
Grade 3	0,48	0,48<1,36

Table 4: Results of K-S test of fit.

and its marginal cumulative density function CDF is:

$$F(x \mid a, b) = \frac{1}{b^a \Gamma(a)} \int_0^x t^{a-1} e^{-\frac{t}{b}} dt \tag{22}$$

where a and b, shape and scale parameters respectively, have the values depicted in Table 5.

Parameters	Grade 1	Grade 2	Grade 3
a	34,582	33,320	28,727
b	0,402	0,407	0,440
μ	13,902 GPa	13,561 GPa	12,639 GPa
σ	2,364 GPa	2,349 GPa	2,358 GPa
$\delta = \sigma/\mu$	0,170	0,173	0,186

Table 5: Parameters of the gamma marginal PDF of the MOE.

4.2 Correlation Function of the Random Field of the MOE

The correlation structure of the random field is described by means of the correlation function. We assumed an exponential correlation function, proposed by Czmoch (1998), based on experimental test carried out in $Pine\ spruce$ timber beams:

$$\rho_{ij} = exp\left(-2\frac{\left|x_c^{(j)} - x_c^{(i)}\right|}{d}\right) \tag{23}$$

where d is the correlation length or scale of fluctuation, which measures the decay of the correlation function, $i.e.$ correlation between values of random field at points separated by greater distance than d, is zero.

In this work, the values considered for the scale of fluctuation of the random field of MOE, are presented in Table 6.

In his work, Czmoch (1998) experimentally found that the scale of fluctuation of the MOE for $Pine\ spruce$ timber beams, is approximately 1,4 m for the serviceability load level, and around to 0,7 m for a load level close to the load carrying capacity. The limit values proposed in this work, correspond to the following cases: d=0, each beam element take a value of E_i

d_0	d_1	d_2	d_∞
0	0,672 m	1,344 m	$\rightarrow \infty$

Table 6: Values of the scale of fluctuation d.

independently from each other, obtaining a set of independent random variables. There is not a real case. $d \rightarrow \infty$, the random field becomes fully correlated and it can be interpreted as a random variable in the limit. It represents a beam with homogeneous MOE. This case is used in reliability studies and in design practice.

Intermediate values shown in Table 6 represent real situations. The scale of fluctuation of the random field d is a very important measure of the correlation, since it governs the optimal size of a random field mesh. Der Kiureghian and Ke (1988) have shown for the midpoint method with the exponential correlation function, that a sufficiently accurate value of the reliability index is obtained if the random field element size is between one-half and one-quarter of the scale of fluctuation. Results presented in this work has been obtained with elements shorter than one-quarter of d.

4.3 Application of Nataf Transform

Applying the correlation function, Eq. (23), the correlation matrix R is obtained. Then, Nataf transform is employed to find the correlation matrix R_0. The components of this matrix are related through the next equation, Der Kiureghian and Liu (1986):

$$\begin{aligned} \kappa = \frac{\rho_{0ij}}{\rho_{ij}} &= 1,022 + 0,022\rho_{ij} - 0,012(\delta_i + \delta_j) + 0,001\rho_{ij}^2 + 0,125(\delta_i^2 + \delta_j^2) \\ &- 0,077\rho_{ij}(\delta_i + \delta_j) + 0,014\delta_i\delta_j \end{aligned} \tag{24}$$

where δ_i and δ_j are the coefficients of variation presented in Table 5, in our case $\delta_i = \delta_j$. This expression constitutes the solution to the Eq. (18).

Next, once that the correlation matrix R_0 is obtained, the Cholesky decomposition is applied to give the lower triangular decomposition of R_0. This is possible, due to the correlation matrix R_0 is positive-definite. Then, applying this lower triangular matrix to a vector of uncorrelated samples, generated by means of independent Monte Carlo simulations, sample vector with the covariance properties of R_0 is produced. Finally, to obtain samples of the random field of MOE, with the covariance properties of R, Eq. (12) is applied.

5 NUMERICAL RESULTS

5.1 Numerical Simulation of timber beams subjected to pure bending

In this section, numerical results are presented. In this first part, results of midspan deflection of simply supported $Eucaliptus\ grandis$ timber beam, subjected to pure bending are reported. The data of the simulation is depicted in Table 7.

These dimensional parameters correspond to timber beams of structural size, that are often used in design practice. The applied bending moment was chosen, in a way that the material works in the linear elastic range.

Taking into account the limits established previously, related with the mesh of random field, and in order to obtain a good representation of the random field of MOE, we adopted 40 beam elements. In Figures 4-6, a convergence study is shown, where N° is the number of independent Monte Carlo simulations. The results of the convergence study, correspond to limiting and

Parameters	Values
Lenght	2 m
Nominal section	45 x 120 mm
Second moment of area	0,5765 x $10^{-5}\mathrm{m}^4$
Applied bending moment	604,5 Nm
Eucalyptus grandis	Grade 1 ($cf.$ Table 5)

Table 7: Parameters used in numerical simulation.

intermediate values of d. Fast convergence is observed for the mean value (E[V(L/2)]), Figure 4, percentile 90 % (P90[V(L/2)]), Figure 5, and standard deviation (σ[V(L/2)]), Figure 6, for lower values of d. The number of simulations that gives a reasonable accuracy, increases with the increase of d.

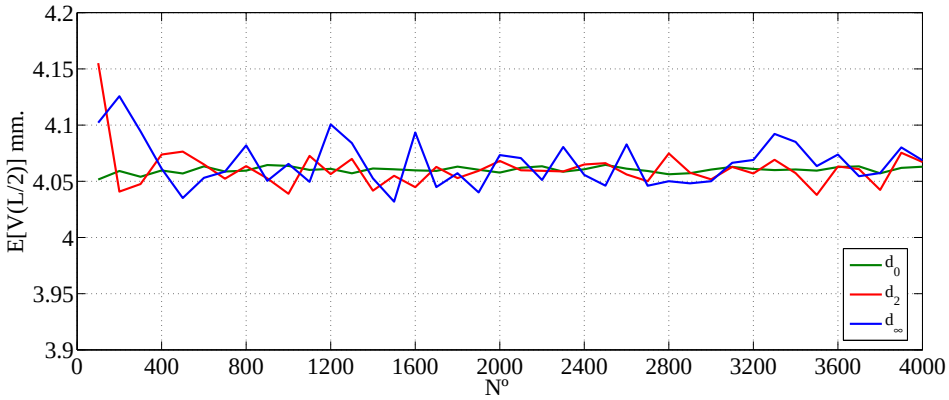

Figure 4: Convergence of the mean values E[V(L/2)] for different values of the scale of fluctuation.

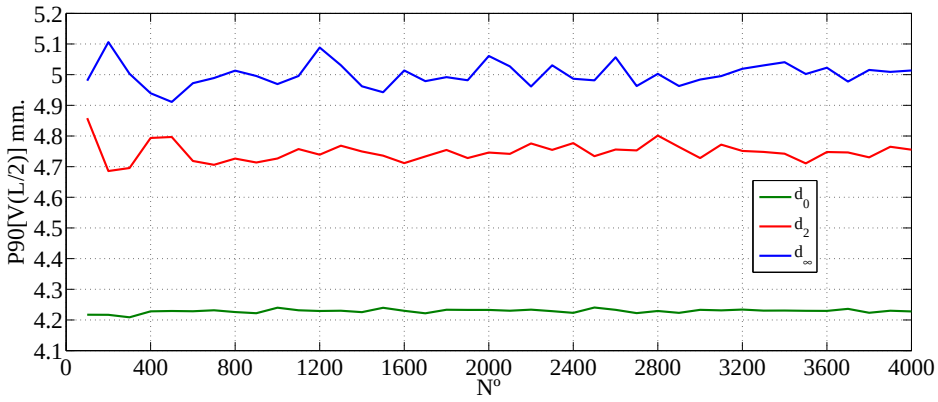

Figure 5: Convergence of percentile 90% of F[V(L/2)] for different values of the scale of fluctuation.

As can be seen in the figures previously presented, an acceptable convergence is achieved when N°= 2000 for all values of d. Next, for this number of independent Monte Carlo simulations, the PDF and CDF of midspan deflection (f[V(L/2)] and F[V(L/2)]) are obtained. Figure 7 shows the PDF and CDF of V(L/2) and the influence in the response of the scale of fluctuation d. Furthermore, it can be seen that the mean values of the response remain approximately equal, for all values of d. It can be also observed that an increase of the value of d, produces an

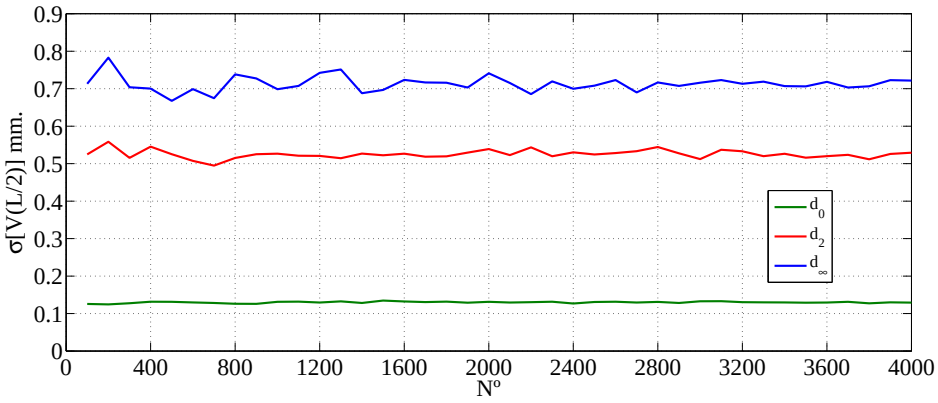

Figure 6: Convergence of the standard deviation $\sigma[V(\text{L}/2)]$ for different values of the scale of fluctuation.

increase in the standard deviation of the f$[V(\text{L}/2)]$. This behavior also can be viewed in Figures 4-6. This means that a homogeneous beam presents higher values of deformation than a inhomogeneous beam, and also shows a large variation or dispersion from the average or expected value of $V(\text{L}/2)$.

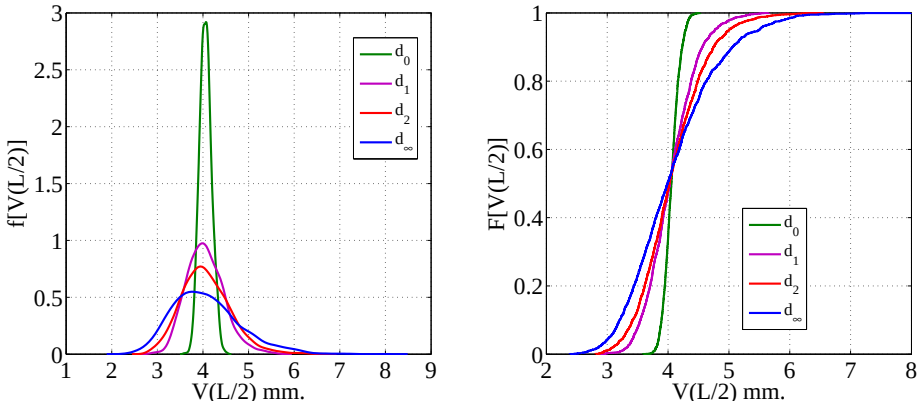

Figure 7: PDF and CDF of $V(\text{L}/2)$ for different values of the scale of fluctuation.

In Figure 8 and Table 8, the influence of d in the upper percentiles of F$[V(\text{L}/2)]$ can be observed. This values, for the upper percentiles, are important to obtain characteristic values of midspan deflection applied to the reliability study of timber beams. As can be seen in Table 8, when $d \to \infty$, the response is higher than in the realistic model of longitudinal variation of MOE. In Figure 9 some realizations of the random field are shown.

d=0	d=0,672 m	d=1,344 m	$d \to \infty$
4,23 mm	4,56 mm	4,74 mm	5,06 mm

Table 8: Percentile 90 % of F$[V(\text{L}/2)]$ for considered values of d.

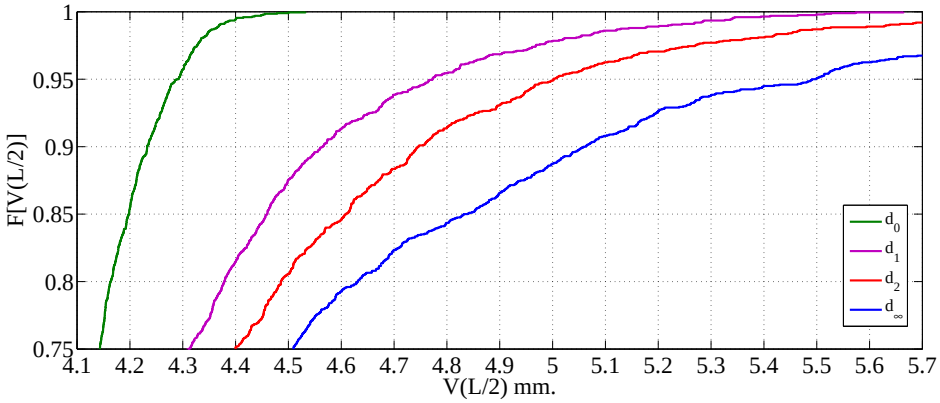

Figure 8: Influence of the scale of fluctuation in the upper percentiles of F[V(L/2)].

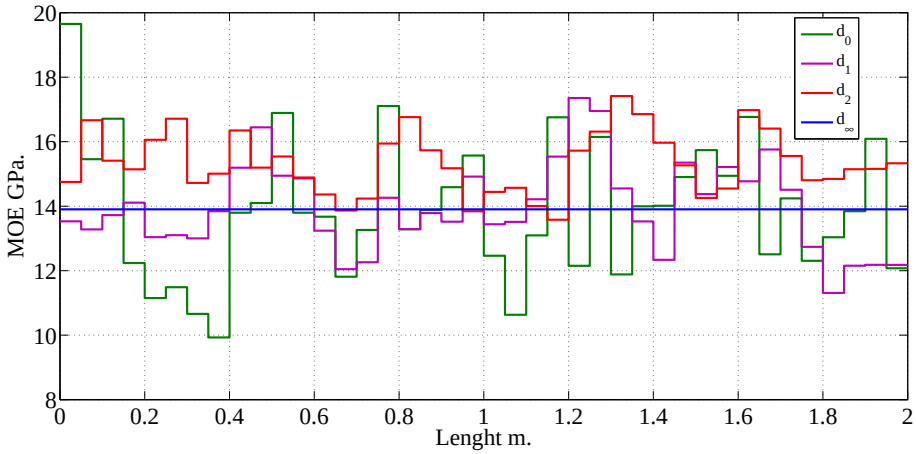

Figure 9: Some realizations of the random field $E(x)$ for different values of the scale of fluctuation.

In the next section, the limit case when $d \to \infty$ ($i.e.$ homogeneous MOE in the beam), is studied. In order to find the PDF of midspan deflection analytically, the theorem of change of variables is applied. The probability of finding a value of the random variable X between a and b is:

$$P(a < X < b) = \int_a^b f(X)dX \tag{25}$$

Then the following theorem applies:

Let X be a continuous random variable with PDF $f(X)$. Let us define $u = \phi(X)$ and the inverse function $X = \Psi(u)$. Then the PDF of u is given by $g(u)$ where

$$g(u)\,|du| = f(X)\,|dX| \tag{26}$$

$$g(u) = f(X)\left|\frac{dX}{du}\right| = f(\Psi(u))\,|\Psi'(u)| \tag{27}$$

The application of this theorem to the midspan deflection when $d \to \infty$, case of fully correlated MOE of timber beam, yields:

$$V\left(\frac{L}{2}\right) = \frac{\mathcal{M}}{EI}\left(\frac{L^2}{8}\right) = \frac{N}{E} \tag{28}$$

solving Eq.(2). Then:

$$g(V) = f(E)\left|\frac{dE}{dV}\right| = f\left[\frac{\mathcal{M}}{VI}\left(\frac{L^2}{8}\right)\right]\left|-\frac{\mathcal{M}}{V^2 I}\left(\frac{L^2}{8}\right)\right| = f\left(\frac{N}{V}\right)\left|-\frac{N}{V^2}\right| \tag{29}$$

$$g(V) = \frac{\left(\frac{N}{V}\right)^{a-1} e^{-\frac{\left(\frac{N}{V}\right)}{b}}}{b^a \Gamma(a)}\left|-\frac{N}{V^2}\right| \tag{30}$$

Eq. (30) is the PDF of midspan deflection when $d \to \infty$. Figure 10, show a comparison between the histogram obtained with 2000 independent Monte Carlo simulations and the histogram obtained from the analytical expression Eq. (30). As can been seen in Figure 10, numerical results converge to the analytical expression obtained previously via the change of variable. The $ksdensity(x)$ function of MATLAB that computes a probability density estimate of the sample in the vector x was used to find the numerical PDF.

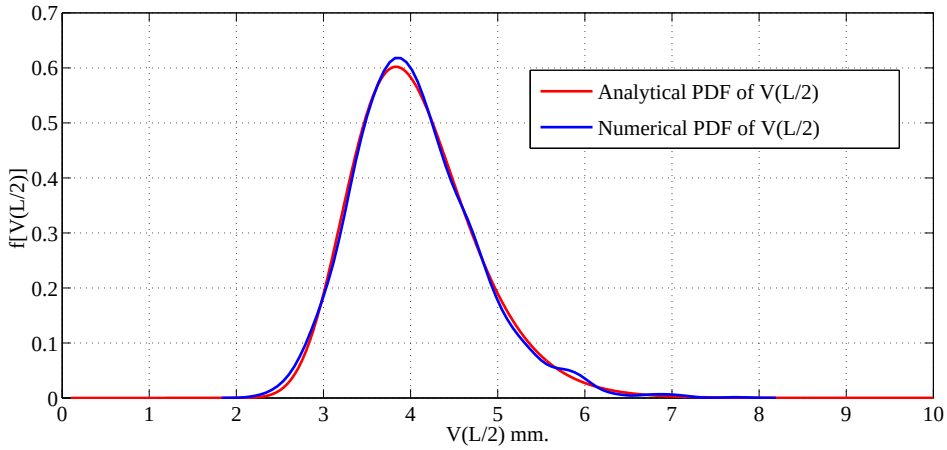

Figure 10: Comparison between numerical results and analytical expression of midspan deflection.

5.2 Numerical Simulation of Experimental Bending Test

In this section, a comparison between numerical and experimental results of the midspan deflection is presented. Experimental data of the midspan deflection, obtained by means of a two point loads bending test, performed with 50 sawn beams of Argentinean *Eucalyptus grandis*, with a nominal section of 50 x 75mm, are employed. Experimental bending tests were carried out according to UNE-EN408 (1995), Figure 3, and the worst defect were placed in the constant bending zone, between two concentrated loads and in the tensile region of the cross section.

The tested beams belong to the following strength classes, according to IRAM:9662-2 (2006), Table 9.

Strength class	Number of tested beams
C1	19
C2	9
C3	22

Table 9: Classification of tested beams.

Parameters employed in numerical simulations are depicted in Table 10.

Parameters	Values
Lenght	1,19 m
Nominal section	50 x 75 mm
Real section	41,89 x 66,49 mm
Second moment of area	1,0261 x $10^{-6}\mathrm{m}^4$
Applied force	900 N
Eucalyptus grandis	Grade 3 (cf.Table 5)

Table 10: Parameters used in the numerical simulation.

As can be seen in Table 9, the selected sample was chosen because it has a 56 % of high quality structural timber. On this base, in what follows, we explain the influence of this choice in the results that are shown below. Dimensional parameters correspond to averages values obtained from the 50 tested timber beams.

A numerical study was carried out, discretizing timber beams with 18 beam elements and 2000 independent Monte Carlo simulations. In Figure 11, a comparison of numerical and experimental PDF and CDF of the midspan deflection is shown. In the lower part of the experimental CDF (under 50%), results are located among numerical CDF. One possible explanation of this result could be that the midspan deflection of beams with higher stiffness and lower number of defects are found in this region. The numerically found CDF differs with the experimental curve in the upper part of the plot. Here the beams probably have a larger number of defects and more, the numerical model does not account for knots and pith ($e.g.$ C3 beams). Numerical results are acceptable and show a good prediction of midspan deflection of the tested sample. This comparison can not accurately predict the value of the scale of fluctuation of *Eucalyptus grandis* beams. To make this possible it would be necessary to run an experimental program.

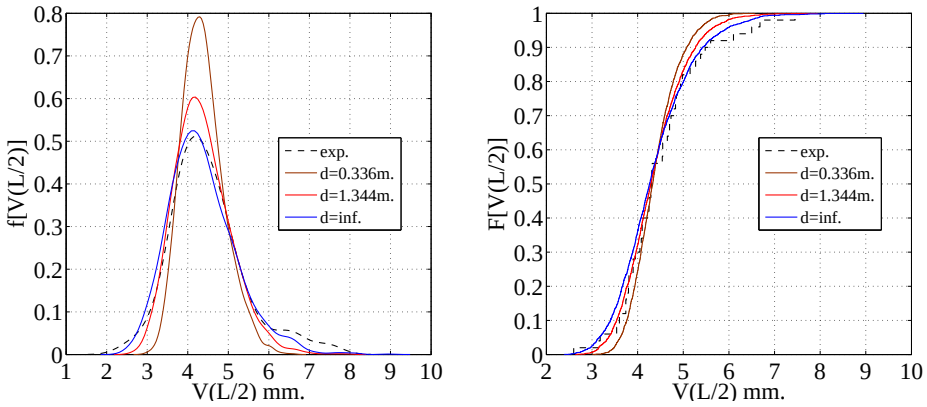

Figure 11: Comparison between numerical and experimental PDF and CDF.

6 CONCLUSIONS

The PDF and CDF of the midspan deflection of timber beams, with uncertain material properties, were obtained. The stochastic analysis allows to obtain more information of the structural components behavior. The influence in the response of the scale of fluctuation was presented. Numerical simulation of beams with higher values of scale of fluctuation ($i.e.$ homogeneous

MOE model) present upper percentile values of the midspan deflection higher than the realistic model. They also present higher values of the standard deviation in the PDF of the midspan deflection. Therefore, the MOE modeled as a random variable constitutes a conservative approach and is on the safe side.

Results of numerical simulations of bending tests were also presented. They show, that numerical simulations with the MOE represented as a random field provide results close to the experimentally obtained, inasmuch as timber beams are of superior quality. The difference between numerical and experimental results is influenced by timber defects which the numerical model does not include, such as knots and presence of pith.

The lengthwise variability model of the MOE presented is applicable to several load cases and constitutes a more realistic material approach, applicable to reliability studies of serviceability limit states of structural components made of $Eucalyptus\ grandis$ timber.

REFERENCES

Bathe K.J. *Finite element procedures*, volume 1. Prentice hall Englewood Cliffs, 1996.

Benjamin R.J. and Cornell C.A. *Probability, Statistics and Decision for Civil Engineers*. McGraw-Hill, 1970.

Czmoch I. *Influence of structural timber variability on reliability and damage tolerance of timber beams*. Ph.D. thesis, Luleå tekniska universitet, 1998.

Der Kiureghian A. and Ke J.B. The stochastic finite element method in structural reliability. *Probabilistic Engineering Mechanics*, 3(2):83–91, 1988.

Der Kiureghian A. and Liu P.L. Structural reliability under incomplete probability information. *Journal of Engineering Mechanics*, 112:85–104, 1986.

Ditlevsen O. and Madsen H.O. *Structural reliability methods*, volume 178. Citeseer, 1996.

Escalante M.R., Rougier V.C., Sampaio R., and Rosales M.B. Buckling of wood columns with uncertain properties. *Mecánica Computacional, Volume XXXI. Number 14. Uncertainty and Stochastic Modeling*, pages 2735–2744, 2012.

INTA. *Manual para productores de eucaliptos de la Mesopotamia Argentina*. INTA, 1995.

IRAM:9662-2. Madera laminada encolada estructural. Clasificación visual de las tablas por resistencia. Parte 1: Tablas de Eucalyptus grandis . *Instituto Argentino de Racionalización de Materiales IRAM, Buenos Aires*, 2006.

Isaksson T. *Modeling the Variability of Bending Strength in Structural Timber: Length and Load Configuration Effects*. División of the Structural Engineering, Lund University, 1999.

Köhler J. *Reliability of timber structures*. 301. vdf Hochschulverlag AG, 2007.

Köhler J., Sørensen J.D., and Faber M.H. Probabilistic modeling of timber structures. *Structural safety*, 29(4):255–267, 2007.

Piter J. *Clasificación por resistencia de la madera aserrada como material estructural. Desarrollo de un método para el Eucalyptus grandis de Argentina*. Ph.D. thesis, Tesis Doctoral. Universidad Nacional de la Plata, 2003.

Rubinstein R.Y. *Simulation and the Monte Carlo method*. John Wiley and Sons, Inc., 1981.

Shannon C. A mathematical theory of communication. *The Bell technical journal*, 27:379–423, 1948.

UNE-EN408. Estructuras de madera. Madera aserrada y madera laminada encolada para uso estructural. Determinación de algunas propiedades físicas y mecánicas. *Estructuras de Madera, Editado por AENOR-Asociación Española de Normalización y Certificación, Madrid*, 1995.